ГЛАСНИК Српског географског друштва 99(1) 45-68
BULLETIN OF THE SERBIAN GEOGRAPHICAL SOCIETY 2019

Original scientific paper
UDC 332.368 : 001.89
https://doi.org/10.2298/GSGD1901045D

Received: April 3, 2019
Corrected: April 29, 2019
Accepted: May 12, 2019

József Denső[1*], Amadé Halász[**], Viktória Poór[*], Dénes Lóczy[*]

[*] *University of Pécs, Faculty of Sciences, Hungary*
[**] *University of Pécs, Faculty of Medicine, Hungary*

SCREENING OF POLLUTION FOR THE RECLAMATION OF INDUSTRIAL LAND: EVALUATION OF GEOLOGICAL BACKGROUND DATA

Abstract: The paper focuses on the results of rapid, combined multi-techniques in field measurements influenced by the geological background, which allow the survey of extensive polluted areas and decision support systems. The investigated area (former briquette factory) is highly contaminated by Total Petrol Hydrocarbon-types (TPHs). Heavy metals were investigated with GC-MS, turbidimetric, Raman-spectroscopic method, and with XRF. Qualitative assessment of alkanes, alkenes and alkines as well as aromatic compounds was determined by Raman peak analysis. The areas contaminated with Cr, Zn, Co and carcinogenic hydrocarbons, are in most cases absorbed in the coal powder matrix.

Key words: environmental assessment, TPH, metal contamination, Raman spectroscopy, gas chromatography, industrial area.

[1] dejozsi@gamma.ttk.pte.hu (corresponding author)

Introduction

Application of rapid techniques in contaminated fields

The utilisation of solid fossil fuels involves several types of pollution, the survey, study, mitigation and possible reclamation of which is a crucial environmental problem. TPHs (Total Petrol Hydrocarbons), and heavy metal (Co, Pb, As, Zu, Cr, Ni, etc.) contaminations affect areas all around the World due to long term coal mining and briquette factories operation (Rainbow, 1990; Panov et al., 1999; Cicek & Koparal, 2004; Lóczy et al., 2007; Dick et al., 2006), or cause different kinds of medical problems (Ahern et al., 2011). At the same time, these fuels are indispensable for human society and cannot be substituted by others (Coal Fact reports 2012-2014, Haibin & Zhenling, 2010).

Coal-based electricity generation takes place on large scales particularly in rapidly developing economies, such as China and India. The ecological footprint of coal-based industrial and energetic activities is among the highest. In the assessment of environmental impact, rapid field measurement techniques are useful since this way high-resolution information can be obtained on the contaminated areas. Remediation can take various directions, including re-utilisation for alternative energetic purposes (Boadi, 2012). Part of the polluted substances of high-energy content can be used in situ as fuel – assuming that they do not contain toxic contaminants in considerable concentration. In most cases, however, they contain other contaminants (such as heavy metals), which induce air pollution and the tail gas treatment technology to be applied during incineration involves too high energy and investment costs.

Environmental screening and determining the spatial distribution of contamination is crucial in the case of most of the environmental problems relates to the disposal of mine waste or abandoned mines, especially the pollution transport pathway (Yenilmez et al., 2011). The wider use of field portable instruments provides an opportunity for fast real-time, cost-effective surveys for the analysis of complex hydrocarbon mixtures and for heavy metal distribution in abandoned areas. The metal contamination on-site is often measured by portable X-ray fluorescence spectroscopy (Powell et al., 2015, Kalnicky & Singhvi, 2001; David et al., 2013). It is also used for on-site soil analysis for standard soil samples (VanCott et al., 1999). The common method used to measure the contaminants from different groups is the gas chromatography (GC). The GC-MS method does not separate the naturally occurring compounds which derive from non-petroleum sources. Therefore, non-petroleum compounds generally cause positive error during the laboratory measurements. Individual batches of petroleum products are mixtures of a large number of compounds and often do not fit into precise categories selected for the standard regulation (Zemo et al., 1995).

Raman spectroscopic monitoring has been performed on diesel particulate matter in coal mines, gasolines (Lyon et al., 1998). Cooper et al. (1997) made a comparison of the three most commonly used vibrational analyses. In general, the standard errors for mid-IR models are slightly lower than for Raman models. As opposed to IR spectroscopy, Raman vibration does not depend on temperature and the moisture content of the sample. Both methods (IR and Raman spectroscopies) supplement each other and their parallel utilisation is more and more common. Although *in situ* measurements the interpretation of peaks is not easy because of the different geological backgrounds.

Crude oil and coal deposits contain PAHs (Castiglioni et al., 2004). The PAHs detection is commonly made by Raman spectroscopic method (Pfannkuche et al., 2012). The various Raman spectroscopy techniques proved to be very valuable in obtaining fingerprints of a wide variety of chemical and biological hazards (Izake, 2010). Using appropriate standards, the Surface enhanced Raman spectra (SERS) method is also suitable for the identification of very low (sub ppm) amounts. The SERS spectra of PAH standards and asphaltene (measurements described by Bowden et al., 2015), where 514 nm was determined on gold substrate in the sub ppm province – much below the exication.

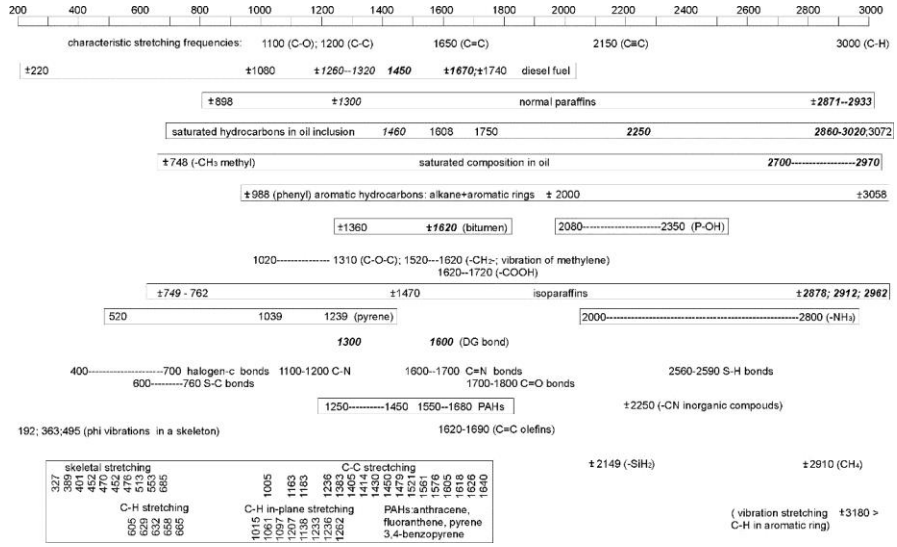

Fig. 1. Summary of the characteristic Raman peaks of hydrocarbon types after Tommasini & Zerbi, 2010, Silva et al., 2011, Zhang et al., 2007, Kolomijeca et al., 2011, Burke, 2001, Leyton et al., 2005

Investigated area

The case study of the subject area is the (former) industrial zone near Nagymányok, located in a northern valley of the Eastern Mecsek Mountains (Southern Hungary) (Fig. 2).

Many authors (Nagy, 1971, Némedi Varga, 1987 and Somos, 1965) described the geology of Eastern Mecsek region. Their works focused mainly on the geological description of coal seams. With abandoned but not rehabilitated buildings, the Nagymányok area represents a potential source of contamination to the living stream flow through the industrial zone, and to the protected subsurface aquifers. The contaminants can migrate into the water and will accumulate in the sediments and mainly in the soil. Three different geological formations can be found in the investigated area (Haas et al., 2010), two of them on the surface. South from the industrial zone in the valley, the Misina Group (limestone) and around the area the younger Pannonian *s.l.* clastic sediments are cropping out. The Mecsek Coal Formation is exposed at more than one km distance from the investigated area. Occasionally, after rainy periods, the forms of hydrocarbon contamination also occur in the surface watercourses of the area. Until the 1990s, this was

the largest briquette factory in Hungary, where the coal powder was cemented by bitumen (Fig. 3).

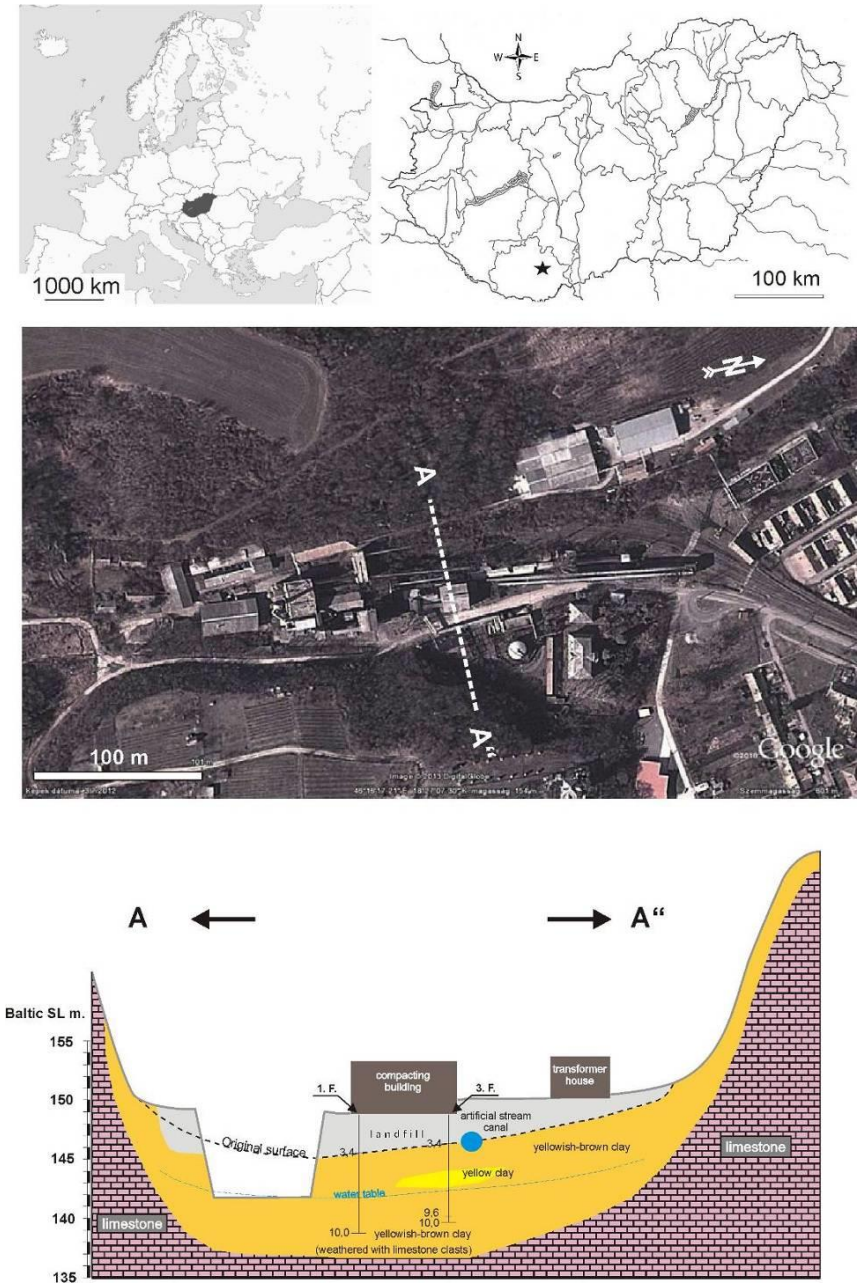

Fig. 2. Location of the study area and its geological cross section (Source: Közkincs, https://commons.wikimedia.org/w/index.php?curid=1467176)

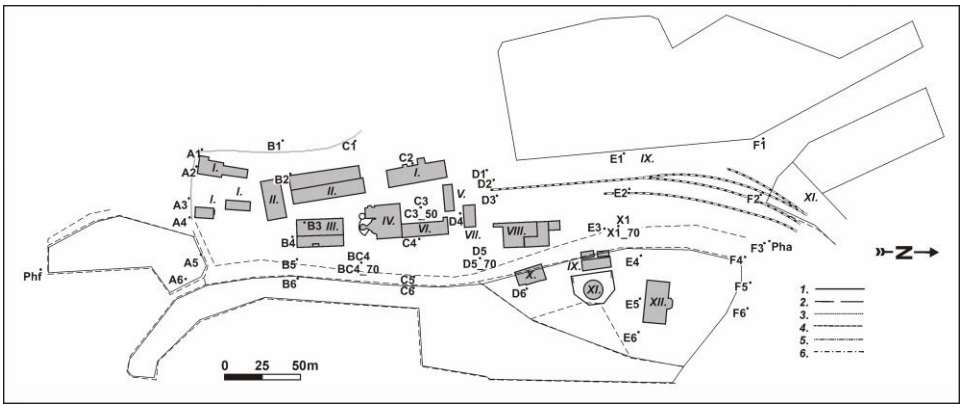

Fig. 3. The former briquette factory

Legend: I - storage units; II - fitting room; III - engine-room; IV - stokehold; V - coal-bunker; VI - dryer; VII - coal-preparatory; VIII - briquette-press; IX - pump-stations; X - transformer station; XI - Bitumen tank; XII - offices; B6 - sample codes and sites; 1 - border of the factory; 2 - subsurface electrical cable; 3 - aerial cord; 4 - potable water pipe; 5 - sewer pipe; 6 - rainwater pipe; A1...F6 sampling sites

Today the demolition works are still incomplete, the remnants of a demolished building (bricks and concrete fragments) and non-demolished concrete structures are left behind. During the investigation, we found at least, four buildings and their environments are highly contaminated by the different kinds of hydrocarbon: the transformer station, the bitumen tank, the mazut pump station, and the engine shed. A former investigation (Ökoproject Report, 2008) concluded that the area is highly contaminated by TPHs and PAHs and slightly by heavy metals. This study, however, was only based on four samplings.

Aims

The first aim of this investigation was the identification of the sources, types and distribution of the pollution with rapid, portable and complementary techniques. The second aim was to obtain additional information on petroleum hydrocarbons using and combining spectroscopic and chromatographic methods (Raman and GC-MS). This study suggests that in situ fingerprint characterization and evaluation of petroleum hydrocarbons lead to cost-effective investigation and more detailed mapping supported by a huge database.

Materials and methods

Legislative background

During environmental screening, chemical analytical methods were applied. The limit values of the contamination can be reliably identified with the applied techniques. Although the limits differ from country to country (Carlon, 2007), the Directive 2006/118 /EC of the European Parliament harmonize them. For the study area the Hungarian standards has to be followed: KöM-EüM-FVM-KHVM Decree No. 10/2000. (VI.2.) on quality standards of groundwater and geological agent protection and the Decree of the

Ministry of Environment and Water, Ministry of Health and Ministry of Agriculture No 6/2009. (IV.14.) KvVM-EüM-FVM.

Sampling

Our sampling sites were selected on the basis of the source of the contaminations and then we covered the whole area in equal distribution. The samples were collected from the vicinity of the production buildings, contain coal (residues of the industrial process), degraded soil types (rendzinas, young fluvial soils), sapropels, sand and gravel particles.

Around the buildings and the railways, the samples contain mainly or entirely coal. For analytical purposes, the majority of the samples were obtained from the surface (10-30 cm). An excavator dug additional three test pits (to a maximum depth of 100 cm; BC4, D5, X1). The location of the samples and the test pits were influenced by the extension of the concrete-covered surfaces; consequently, the regular net-pattern sampling system was impractical and non-feasible. Two sludge samples (PHF, PHA) were collected from a small creek, which flows across the contaminated area through the covered canal (inflow, outflow).

Along the upper course of the stream, channel deposits derive from rocks of the Misina Group and the loess mixed with them. In the northern part of the study area (i.e. along the lower course), they consist of Pannonian sediments. Other siliciclastic sediments are mixed with construction rubble and residual coal powder. From the aspect of the investigation, with regard to the measurement technique, they constitute background conditions, similarly to the natural geological (in situ) background.

From the abandoned barrels and other containers we could sample some hydrocarbon materials, formerly used locally (crude oil, mazut, diesel oil, paraffin-crude oil petroleum and petrol). Although they have been degraded over the years, they are regarded as initial types of pollution.

Methods

For the estimation of the volume of contaminated soils, artificial material, the morphological map of the area and previous technical descriptions of the industrial zone were applied. The schema of the investigation is shown on Fig. 4.

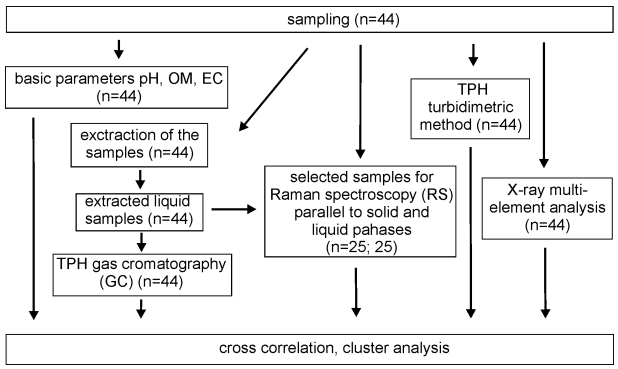

Fig. 4. Flow chart depicting the sampling, investigation and the data fusion procedure.

The pH and EC values were measured by WTW 315 with combine electrode using Metrohm electrode (USDA 2004). Loss on ignition (LOI) analysis is used to determine the organic matter content (%OM). For this purpose, the samples were measured by gravimetric method after ignition at 550°C for 2-4 hours, using a heating block.

The hydrocarbon contamination of soil samples were analysed using three different methods. The PetroFlag test (US EPA Method 8015) determines the quantitative TPH (Total Petroleum Hydrocarbons), based on turbidimetric approach.

The GC-MS device Agilent 6890N gas chromatograph (GC) and 5975 mass spectrometer (MS) for a qualitative analysis were carried out for total petrol hydrocarbon (TPH) measurement according to the ISO 16703:2004 standard. After the sample preparation process 1 µl sample was injected in split mode (split ratio 1:15) with an automatic sampler. The injector temperature was 300°C. The temperature for GC oven was initially set at 50°C for 3 min, than ramped to 300°C at 10°C /min and held for 25 min. The separation was achieved on a HP-1 ms capillary column (25 m x 0,2 mm i.d.x. 0.33 µm film thickness). The flow rate of the carrier gas (helium) was 1,5 ml/min. The analysis were carried out in scan mode. The MS source temperature and quadruple temperature was 230°C and 150°C, respectively. The electron ionisation mass spectra were recorded at 70 eV. Hydrocarbon standards (C_8-C_{14}), diesel oil and mazut samples were used for qualitative analysis.

The Ocean Optics Raman spectrometer was used to determine a "fingerprint" of the hydrocarbon contamination, initial contamination types and background. Raman spectroscopy (using 785 nm 200-450 mW output laser source) was used at 200-400 ms integration time. Raman spectra were collected directly from surface of the sample and by sampling through the walls of the glass vials. For the evaluation and classification of the explanation of the Raman peaks we revised from the literature; the obtained peaks demonstrate different kind of basic hydrocarbon groups).

The Raman spectroscopy analyses provided qualitative results for the samples. Two Raman spectroscopical measurements were taken on each sample: one on the solid phase, and the second on the extracted/liquid phase. From the liquid phase, a sample was prepared for GC-MS investigation. This was necessary to separate the matrix effect caused on the Raman curves by the geological background from the curves of the extracts prepared for the GC-MS measurement.

In parallel, Raman spectroscopy and GC-MS measurements were made on the initial pollution types (complex hydrocarbons like mazut, crude oil, diesel oil, praffin crude oil, petroleum and petrol) too. The geological background with high organic matter content (recent organic material from soil) and OM from alluvial deposits, which may cause disturbance with the measurements of organic pollutants, were also investigated. The latter included industrial raw materials accumulated in the area, coal and burned coal.

During the screening test, we compared the native pollutant material with the collected solid samples. Therefore, we measured some basic hydrocarbon types, the siliciclastic mixed geological background of the investigated area. Raman spectroscopy provides vibrational information, which is very specific for the chemical bonds in molecules. Hydrocarbon functional groups may be qualitatively identified. It can be used to identify unknown compounds and the technique can therefore be used to study changes in chemical bonding.

The metal contaminations were detected by Thermo Scientific Niton XL3t 600 X-ray fluorescence Analyser (50 KV/100μA, Au X-ray source integration time: 600 sec). Evaluating Raman wavelengths if the signal had a high-frequency noise, the Fast Fourier Transform (FFT) filtering method were used (in Origin Pro8 software environment). A FFT filter performs filtering by using Fourier transforms to analyze the frequency components in the input signal. With the cut-off frequency, the filter removes all the high-frequency noise, leaving the true signal.

The TPH, Cr, Zn, Co distribution maps were drawn by Surfer 10 software, and we used the kriging for gridding method. The statistical analyses were performed by Origin Pro8 software (cross correlation, smoothing FFT method) and by PAST version 2.17c (cluster analysis) software.

Results and discussions

These samples mostly contain mixed materials, i.e. a significant amount of coal powder, loamy deposits and gravel transported to the studied area. Some samples, however, contain in situ developed soils and eolian deposits, primarily loess, and rendzina soils. The results of pH, electrical conductivity (EC) and organic material (OM) measurements can be seen in the Tab. 1.

Tab. 1. The pH, EC and OM values of the samples

Sample code	Ph	EC (μS)	OM (%)	Sample code	Ph	EC (μS)	OM (%)	Sample code	Ph	EC (μS)	OM (%)	Sample code	Ph	EC (μS)	OM (%)
A1	7.45	300	4.5	B6	7.56	410	4.7	D4	7.39	850	91.2	F2	7.72	200	87.4
A2	7.59	390	34.1	C1	7.73	279	6.1	D5	7.45	305	67.8	F3	7.62	360	42.5
A3	7.61	269	25.2	C2	7.73	290	51.2	D5_70	7.48	1390	32.2	F4	7.75	290	18.7
A4	7.61	279	46.8	C3	7.51	2100	87.1	D6	7.48	259	23.2	F5	7.62	290	8.9
A5	7.62	285	12.2	C3_50	7.39	4000	92.3	E1	7.57	220	91.2	F6	7.56	278	4.1
A6	7.59	273	3.4	C4	7.2	6400	81.1	E2	7.5	260	92.3	X1	7.9	330	37.9
B1	7.92	231	2.6	C5	7.84	275	64.1	E3	7.57	1800	34.1	X1_70	7.7	420	27.6
B2	7.73	340	67.1	C6	7.48	390	5.2	E4	7.83	290	23.8	Pha	7.61	330	12.1
B3	7.7	279	28.1	D1	7.46	2300	87.1	E5	7.85	269	21.1	Phf	7.61	360	4.5
B4	7.66	280	35.1	D2	7.64	450	89.1	E6	7.61	290	12.4	CB4	7.57	450	28.8
B5	7.73	282	31.1	D3	7.6	5000	91.1	F1	7.6	195	78.9	CB4_70	7.86	310	34.1

EC depends on water soluble salts. The higher is the proportions of finer particles (clay minerals) and organic matter content in the sample, the more natural dissolved materials and pollutants in the environment are absorbed. Where EC is high (500μS/cm or above), complex pollution types were found and high amounts were measured. The following metals as potential contaminants involving health issues fell into the detectable ranges: Cr, Co, Ni, Cu, Zn, As and Pb (Tab. 2). For a better visual representation, the quantitative results of TPH measurements are also shown.

The most frequent contaminant is the Cr, but this metal has less wide variance related to Zn, which has an extraordinarily wide range. In the further analyses of samples, we intended to identify partial areas according to the amounts and types of pollution. The applied cluster analysis shows which samples (out of all pollution types) belong to the same group (Fig. 5). At the fourth level of hierarchy groups could be identified. Sample C_4 forms a separate group with extremely high Zn contamination. The second group has high Zn and Co values. The third group (from A1 to E5) presents low contamination values

mostly located peripherally in the area. The fourth group comprises the largest number of elements.

Tab. 2. The values of the metal- and TPH

contaminants	Cr	Co	Ni	Cu	Zn	As	Pb	TPH
limit value (ppm)*	75	30	40	75	200	15	100	100
code								
detection limit (calibrated with $Si0_2$)	65	40	50	25	15	9	8	X
A1	60			30	180	10	20	461
A2								362
A3	70	70		40	70	10	40	511
A4	50			30	70	10	20	504
A5	80		20	30	160	10	40	236
A6	70		40	40	90	20	30	57
B1	60			20	50	10	20	123
B2	70		30	40	160	20	60	784
B3	100	330		170	480	20	240	1,677
B4	70		20	40	190	10	50	2,441
B5	70		50	40	70	10	20	776
B6	70	80	30	40	500	20	70	342
C1	60			20	50	10	20	326
C2				30	110		30	1,456
C3	90		60	90	460	30	90	1,128
C4					2,090		50	2,184
C5				30	110		50	67
C6	80	180		50	290	20	90	234
D1	60	90	30	20	50	10	20	47
D2	130			30	160	10	40	2,530
D3	90	90		70	50	20	40	1,876
D4	90			40	100	20	110	56
D5	100			30	90	10	30	2,129
D6	70			20	110	10	30	321
E1	90			20	80	10	50	76
E2	90		40	50	170	10	60	45
E3	60	120		30	50	10	30	1,130
E4	70		20	20	80	10	20	905
E5	110		50	70	260	10	40	529
E6	100	90	30	40	120	10	30	211
F1	90	80		30	110	10	40	31
F2	110		30	50	80	10	30	210
F3	80		0	40	1250	10	40	45
F4	50		40	50	130	10	90	341
F5	80		40	40	90	10	40	2,187
F6	70		40	30	110	10	30	442
Phf	50			20	200	10	50	418
Pha	70	130		30	130	10	40	1,460
BC4	90		30	40	130	20	40	1,169
BC4 70	80		60	60	140	10	50	541
C3 50	60			40	70	10	30	1,526
D5 70	80			40	120		90	1,472
X1					60		30	2,304
X1_70	90			30	80	10	30	2,034
average	78.46	126.	34.74	40.98	186.51	12.63	48.14	856.91
median	80.00	90.00	30.00	40.00	110.00	10.00	40.00	507.5
variance	18.00	78.77	14.67	25.48	316.22	5.03	37.24	793.78

* followed the 6/2009. (IV. 14) KvvM – EüM-FVM hungarian regulation
grey background: over the limit of the regulatilon

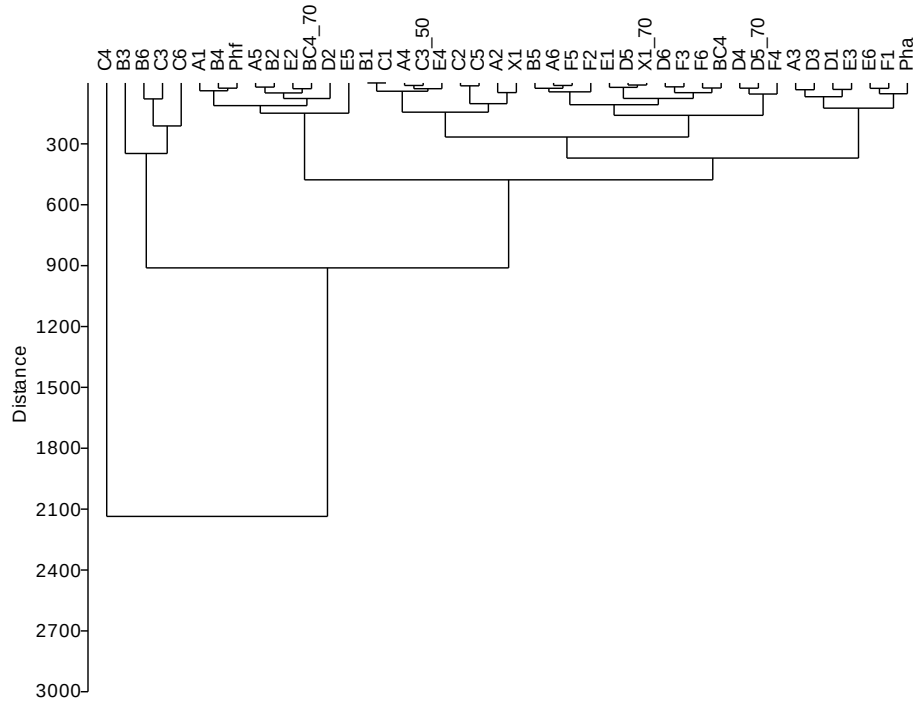

Fig. 5. Cluster analysis (Ward's method) of the heavy metal contamination types

The spatial distributions of the most important contaminants are visualized by the Fig. 6. TPH are present in relatively high concentrations in the area with a more severely contaminated centre. Concentrations of TPH contamination are primarily found along the railway, at pump-stations, E of the briquette-producing unit and at the engine room. Heavy metal contaminations are also located around the central buildings and the briquette factory. At the same time, their spatial distribution is different and makes the planning of mitigation works more difficult. There are areas, which are severely contaminated by a single metal (such as Cr at the NE part or at the end of railway) and others where only TPH contamination is typical. Hydrocarbon contamination can be further subdivided into carcinogenic (PAH, BTEX) and less dangerous (paraffines) components.

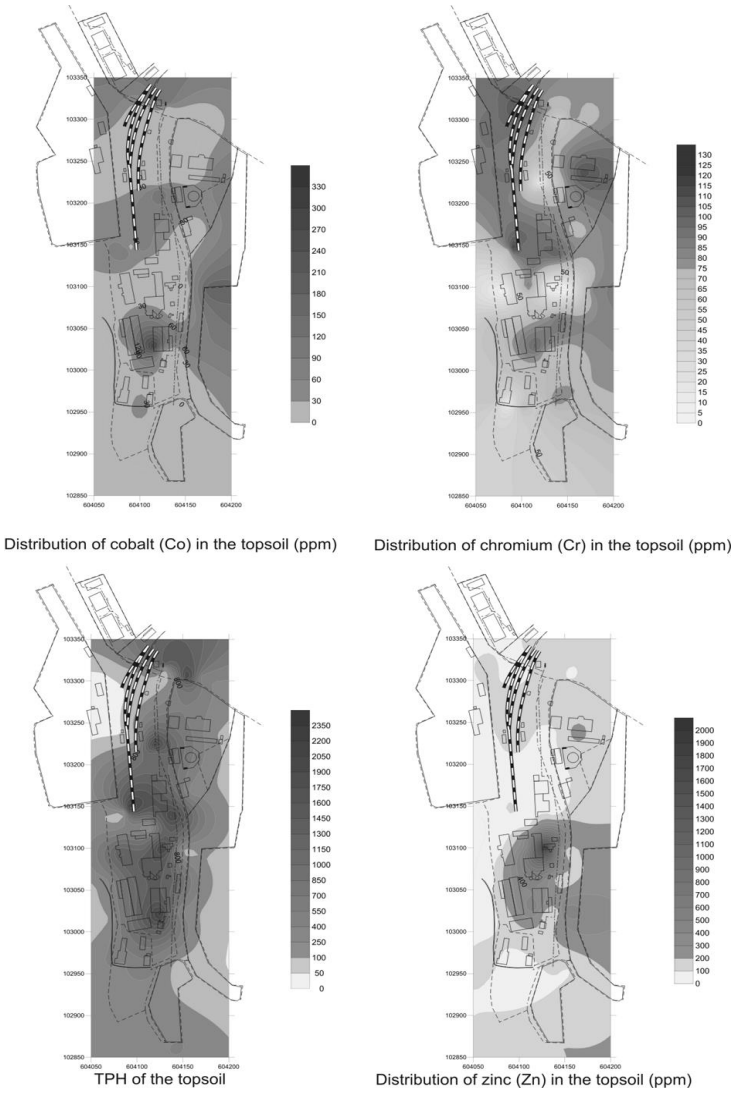

Fig. 6. Co, Cr, TPH, Zn, distribution over the surface (north direction is to the top)

The identification of the hydrocarbon compounds in the soil samples were based on the comparison of GC-MS retention data with standards (alkanes, diesel oil and mazut) and the data of mass spectral libraries have also been used.

The Fig. 7 show the chromatogram of diesel oil, mazut, mixed and mostly heavy oil type sample. The typical carbon range for diesel oil is C_{11} to C_{30} with the majority in the C_{13}-C_{23} range. The typical carbon range for mazut is C_{11}-C_{40} with the majority at C_{18}-C_{30}.

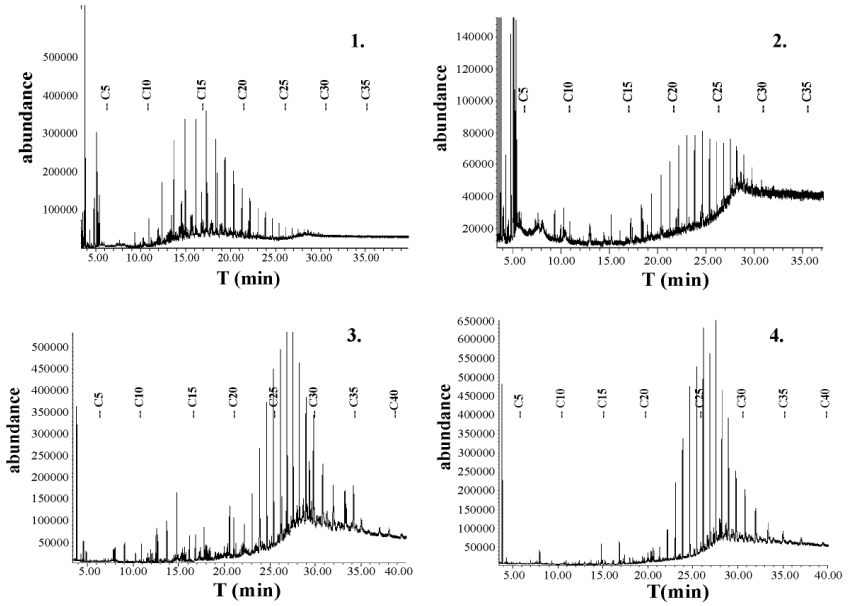

Fig. 7. The gaschromatogram of diesel oil (1), the heavy oil type from mazut (2), mixed (3; Sample X1 70) and mostly heavy oil type contamination (4; Sample PHL)

The diesel, mazut and heavy oil types were the most commonly used materials in this area. These types have a relatively long degradation period. The heavy oil types used in machines, trucks, etc. often contain other additive components, especially heavy metals.

The chromatograms of the extracted soil samples, regarding the major components, were similar in the C_{20}-C_{40} range. In this range, alkanes were detected. Both the number of carbon atoms and the chromatographic patterns refer to typical heavy oil contamination origin. Components also appear under C_{20}, but in these range qualitative differences were found in the samples. Including paired and unpaired alkanes. In some samples, individual peaks are present. In most cases, we could identify mixed and heavy oil–type contaminations.

GC-MS results do not inform about whether the alkanes and alkines in the sample belong to saturated or unsaturated groups. Therefore, the bonding types of coal were identified using Raman spectroscopy.

Raman spectroscopy

Raman spectroscopy began with measurements of initial hydrocarbon pollution types and the organic geological background. The polluting hydrocarbons are themselves very complex compounds, mixed with each other in the contaminated area, degraded and selectively bound to the geological matrix. Therefore, we could not identify precisely the pollutants present, but from the typical vibrational spectra of bond types, the presence of the individual hydrocarbon groups could be identified.

Characteristic Raman peaks associated with specific organic functional groups were analyzed. This information to be used to determine the composition of an unknown

sample containing various functional groups similar to those studied in this lab (Lin-Vien et al., 1991, Lambert et al., 1987)

For smoothing the Raman signals Origin Pro8 signal processing smoothing commands with the Savitsky-Golay and Fast Fourier Transformation (FFT) filters were applied (Fig. 8. a.b.). The same softwares were used for the selection of peaks.

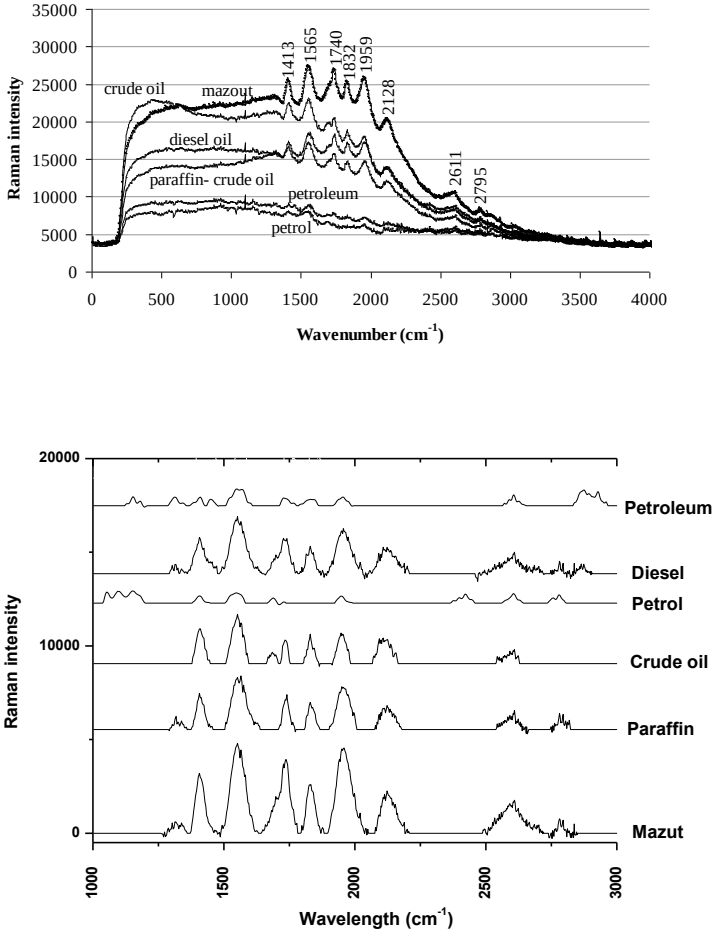

Fig. 8. The raw Raman spectra of the initial contamination types (a) their subtracted shape (b)

Fluorescence at lower wave number (300-1,200 cm^{-1}) is present for all hydrocarbon types, more intensively for cude oil than other marked, easily interpretable peaks. The higher is the ratio of high carbon number components in the investigated material (petrol>petroleum>diesel>mazut), the more characteristic are the Raman peaks. The peaks 1,413 and 1,565 are vibrations of C-C bonds, the peaks 1,740 and 1,832 cm^{-1} indicate C=O stretch bonds, typical of aliphatic aldehides. The peak around 1,959 shows the presence of cycloalkanes, the peak at 2,128 corresponds to the triple bond C≡C characteristic of alkil acethylenes. The component responsible for this peak is probably some material added to mazut or pollutant in the abandoned barrels of the area.

Among the background or "geological" samples, coal, coke, organic matter of local soil (rendzina) and recent alluvium, i.e. the degree of carbonification for the sapropel is variable (Fig. 9). They are also built up of some complex bonding of coal, which is a disturbance during hydrocarbon determination by Raman spectroscopy. This group contains large amounts of Raman vibration-sensible materials found in the samples.

Raman spectroscopy has been applied by several researchers for the measurement of components (e.g. cellulose) of recent organic residues in the mentioned geological bakcground (Schenzel & Fischer, 2004). Natural graphite only shows a single first-order Raman band at 1,578 cm^{-1}. For less ordered carbons, this band is peaked to higher frequencies (1,580-600 cm^{-1}) and an additional Raman band appears near 1,350 cm^{-1} (Kelemen & Fang, 2001). The FT-Raman investigation of softwood lignin pointed out that a skeletal deformation of aromatic rings, substituent groups and side chains between 340 and 1,100 cm^{-1} induced several peaks (Agarwal, 2008). In the measured samples show an identical bimodal fingerprint. The first peak can be detected between 1,331 and 1,385 and the second maximum is present around 1,580 cm^{-1}.

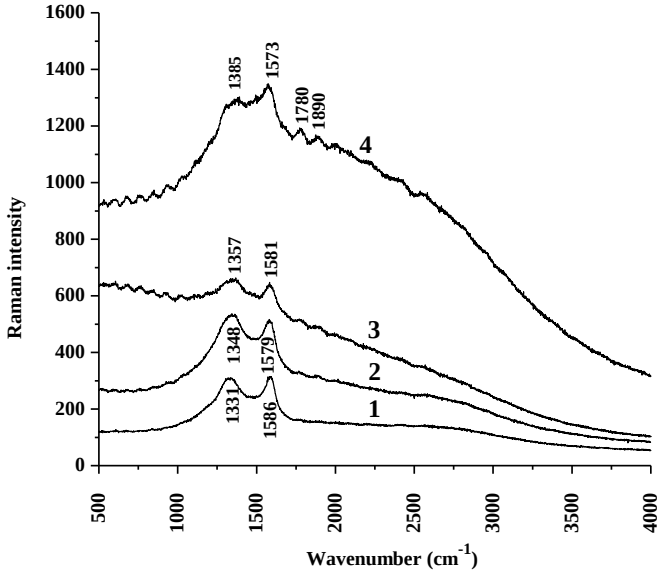

Fig. 9. The Raman peaks of the OM background types (1 coal, 2 coke, 3 recent organic material from soil, 4 OM from alluvial deposit, sapropel)

The Raman spectra (without TPH contamination according the GC-MS investigation) of the mixed artificial and silicastic sample (as frequently background), derived from C_1 sampling site, shows fairly disordered structure (Fig. 10).

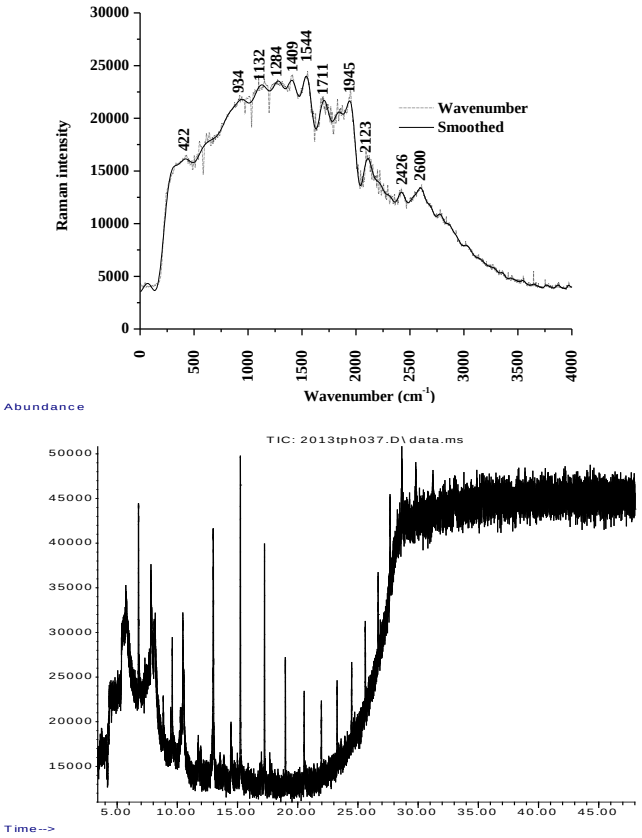

Fig. 10. The Raman spectra of the siliciclastic geological background and GC spectra (mixed artificial and siliciclastic sample), using FFT filtering

At the sample C_3 the major band of quartz 422 cm^{-1} and sulphur 934 cm^{-1}. The calcit and C=S, S=O symmetric stretch show around 1,132 cm^{-1}. 2,123 $-NH_3$ and 2,600 S-H stretch indicates that this sample is not free from organic components. The principal minerals (calcite, quartz, smectites, illite etc.) which build up the loess and Pannonian sediments are mostly swamped. The Raman peaks of the investigated solid samples are shown in Fig. 11.

The Raman intensity of samples grows continually to ca 1,000 cm^{-1}. This is considerably influenced by fluorescence too; therefore, this part lay mostly outside the province of evaluation.

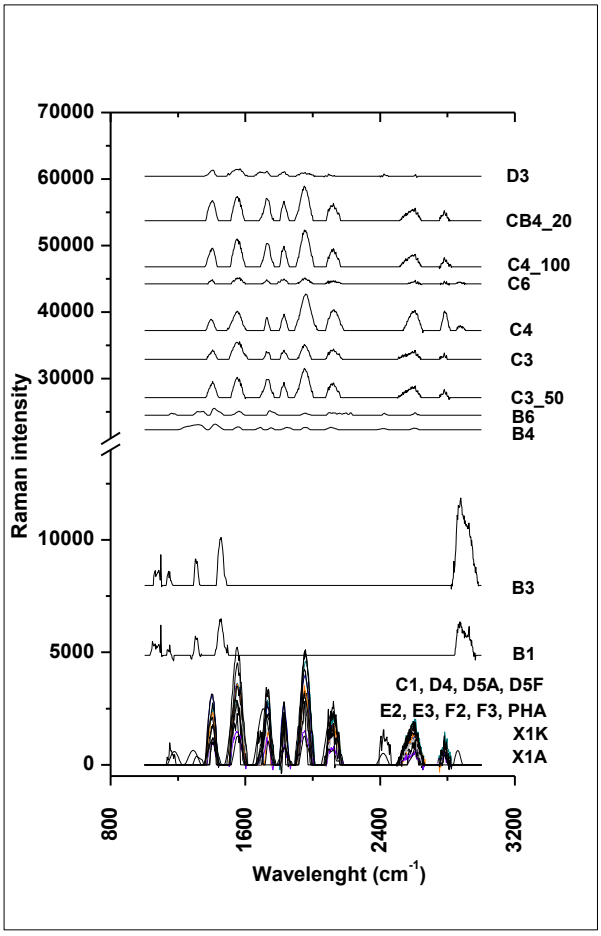

Fig. 11. Raman spectroscopy: through its characteristic vibrational frequencies

The second peak around 1,600 cm^{-1} deriving from the background with high organic matter content (coal powder) is often swamped. Obviously more peaks could be detected which indicate S–H (2,590-2,560 cm^{-1}) C=O (1,700-1,800 cm^{-1}) and C=N (1,600-1,700 cm^{-1}) bonds. The C=O stretch at 1,740 and 1,826 cm^{-1} indicates aliphatic aldehydes. They are also found in processed fossil fuels, hydraulic and transformer oils, and various hydrocarbons. In general, the 1,005–1,300 cm^{-1} province typical of the single C-C bonds, saturated hydrocarbons and aliphatic compounds is less pronounced, but shows a high intensity. At the same time, the peaks also characteristic for initial pollutants (mazut, crude oil, etc.) are distinct. The peaks of the aromatic rings appear characteristically at 1,324 cm^{-1}, 1,416 cm^{-1}, 1,568 cm^{-1}.

Most of the the peaks of the first group has strong similarity to the initial contaminants. The signals from the geological background modified the shape of the curve. They are compared using a cross-correlation table (Tab. 3). The correlation analysis shows high-level similarity (R>0.95) with initial pollutants. This means that based on the statistical comparison, any contaminant can be present in any sample.

Tab. 3. Correlation analysis of pollution types and samples

	Mazut	Petrol	Para-ffin	Crude oil	Diesel	Petro-leum	A2	B1	B3	B4	B6	C1	C3	C350	C4	CB4_20
Mazut	1.00	0.95	0.97	0.97	0.99	0.97	0.99	0.93	0.89	0.97	0.98	0.95	0.93	0.99	0.99	0.99
Petrol		1.00	0.98	0.97	0.95	0.98	0.94	0.91	0.81	0.98	0.97	0.95	0.96	0.97	0.97	0.95
Paraffin			1.00	0.96	0.96	0.94	0.96	0.90	0.95	0.97	0.98	0.98	0.98	0.97	0.97	0.97
Crude oil				1.00	0.95	0.99	0.93	0.88	0.86	0.97	0.94	0.94	0.94	0.98	0.97	0.96
Diesel					1.00	0.92	0.99	0.95	0.90	0.97	0.99	0.97	0.96	0.99	0.99	0.99
Petroleum						1.00	0.90	0.88	0.84	0.98	0.93	0.93	0.93	0.98	0.98	0.93
	CB4_100	C6	D2	D3	D3 coal	D5_70	D5F	D4	E2	E3	X1K	X1A	PHA	PHF	F2	F3
Mazut	0.99	0.92	0.99	0.93	0.89	0.99	0.99	0.99	0.99	0.99	0.99	0.97	0.97	0.99	0.99	0.99
Petrol	0.95	0.97	0.97	0.97	0.89	0.95	0.97	0.97	0.94	0.95	0.96	0.97	0.98	0.97	0.97	0.97
Paraffin	0.97	0.99	0.97	0.96	0.85	0.96	0.97	0.97	0.95	0.96	0.97	0.96	0.99	0.97	0.97	0.97
Crude oil	0.96	0.96	0.97	0.95	0.96	0.96	0.97	0.97	0.93	0.95	0.97	0.99	0.97	0.97	0.97	0.97
Diesel	0.99	0.95	0.99	0.95	0.90	0.99	0.99	0.99	0.99	0.99	0.99	0.95	0.96	0.99	0.99	0.99
Petroleum	0.93	0.95	0.98	0.99	0.95	0.93	0.98	0.98	0.90	0.92	0.91	0.99	0.96	0.98	0.98	0.98

The Raman peaks of the liquid phase provide lower intensity than the solid samples. In this, groups the "pyramid-shape" characterized by geological background disappear. They can be interpreted without processing.

The liquid phase can be divided into two groups. The first group (Fig. 12) is characterized by the typical peaks of the n-alkanes and isoparrafins, such as: 2,850-3,000 cm^{-1} alkanes stretch; 2,882 cm^{-1} symmetric -CH_3 stretch of n-alkanes; 1,465 cm^{-1} –CH_2 – of alkanes). The peak of pi-vibrations of the skeleton range (309 cm^{-1}) and its neighboring appear moderately, which appear at the aromatic rings and/or in the alkenes (olefins).

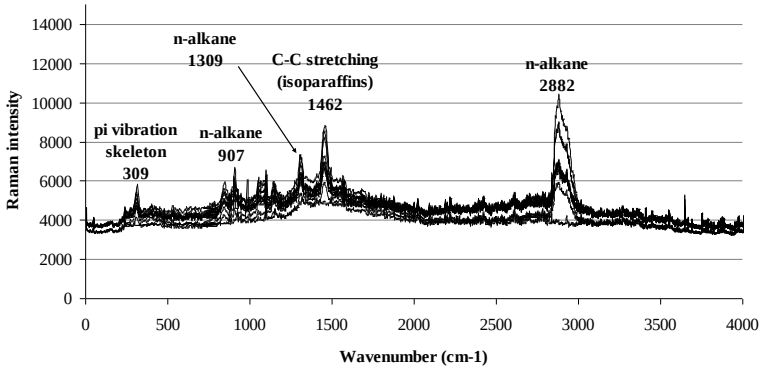

Fig. 12. The first group of the liquid phase (LS1)

The second group (LS2)(Fig. 13) of the liquid phase has a more moderate intensity of vibrational frequencies than the LS1 group (Fig. 12). The pi vibrations range (approx: 300 – 700 cm^{-1} range) rose without peaks due to flourescence. The range of 1,450 – 1,740 cm^{-1} contains more peaks, where mark -CH_2- and C-C band (around 1,465 cm^{-1}). This range may be determined by C=O stretch of aliphatic aldehydes, esters too, the commonly –OH (at 1,740 cm^{-1}) plane could belong to different kind of saturated hydrocarbons,

isoparrafins, the other peaks (2,890-2,940 cm^{-1}) belong to saturated hydrocarbons as well.

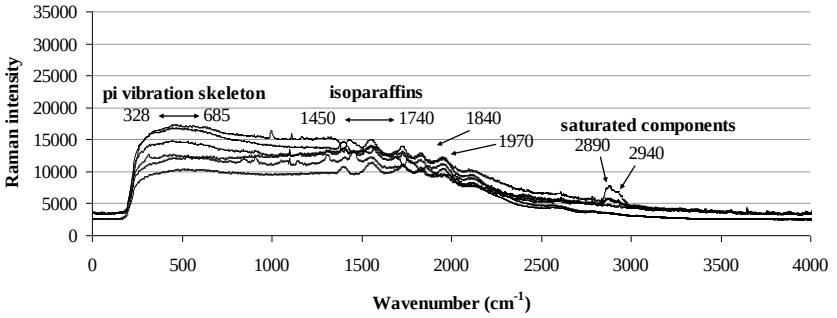

Fig. 13. The Raman peaks of the second group of the liquid phase (LS2) and their cross-correlation

The described statistical groups do not cover all samples; some samples are out of categories. This is explained by the variability of the background reflecting geology and land use. The correlation of measurement results out of category is 0.7 or less, but his does not mean that for such Raman frequencies the identified peaks could not indicate the individual C-C bonds and the qualitative identification of hydrocarbon contamination.

For the interpretation of peaks, i.e. the closer classification of pollution types further information are provided by the joint interpretation of results from solid samples, Raman peaks from fluid phase and GC-MS measurements.

The sample B_4 with 35.12% OM (Fig. 14) is mixed with construction rubble, redeposited loess and loamy alluvial deposits. Its gas chromatogram in the C_{20}-C_{40} province is identical with those of samples in the centre of the area. The alkanes below C_{20} can be detected in smaller amounts since these components have decomposed and evaporated. The peaks marked at 632 cm^{-1} the C-S bond; at 1413 cm^{-1} the anthracene; at 1,568 cm^{-1} the asphaltene and C=C alkenes, at 1,743 cm^{-1} the C=O stretch of aliphatic aldehydes. The curve of the liquid phase marks the (above-mentioned) peaks, which belong to the paraffins.

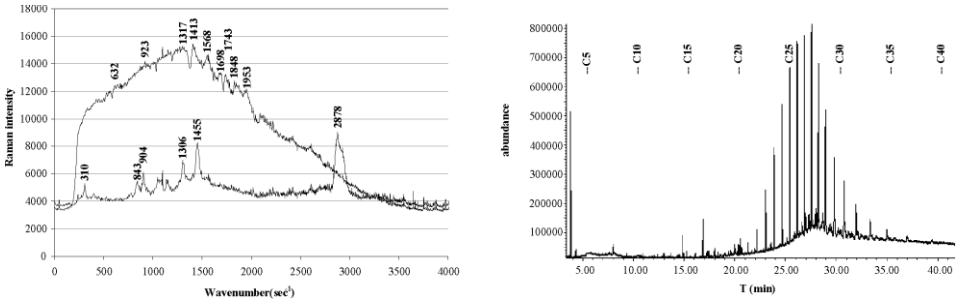

Fig. 14. The Raman peaks of the solid (1) and liqiud (2) phases (a); and gaschromatogram (b) of the sample B4

At the lower part of the investigated area, the canalisated creek leaves the industrial zone. Sample (PHA) which derived from this place contains and sorted fine material, especially fine sand, loam and contains 12.11% OM less than the B_4, therefore the peaks of the vibration are more separated (Fig. 15). Between 200 and 1,400 cm^{-1} the frequencies do not have separated peaks. This interval contains the peaks of the main minerals which establish the creek sediment there are: quartz (470 – 1,350 – 1,596 cm^{-1}), silica (520 cm^{-1}), calcite (279 – 711 – 1,100 cm^{-1}), hematite (225 – 292 – 410 – 612 – 710 cm^{-1}), the strongest peak marked in italics (Raman database). At this sample the peak 462 cm^{-1} refers to quartz. The main important peaks are: at 1,413 cm^{-1} ring stretch of anthracene; 1,551 cm^{-1} benzene derivatives; 1,724cm^{-1} C=O strech; at 1,829 cm^{-1} C=O bond; at 1,956 cm^{-1}, 2,122 cm^{-1} C≡C alkyne and alkyl acetylenes, at 2,612 cm^{-1} C=N bond. In the liquid phase, the 1,321 and 1,466 cm^{-1} belong to the alkanes – CH_2- and around the ~2,899 cm^{-1} double peak is the symmetric and anti-symmetric stretch.

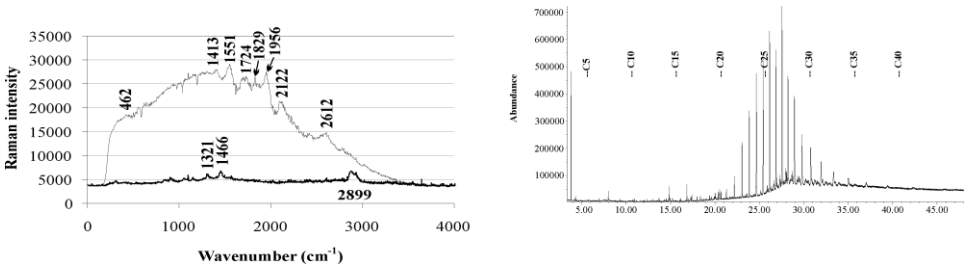

Fig. 15. The Raman peaks of the solid (1) and liqiud (2) phases (a); and gaschromatogram (b) of the sample PHA

Sample C_{3_50} derives from 50 cm depth, the sampling site is in the immediate vicinity of the briquette factory, where contamination is of the highest level (Fig. 16). For samples where the GC-MS analysis pointed out components below C_{20} carbon atom number characteristic peaks occur at the 1,400-2,200 cm^{-1} interval. In addition to the peaks mentioned at the previous samples (1,406, 1,565, 1,727, 1,959, 2,122) the peak at 2,795 cm^{-1} indicates O-CH_3. The lighter components are interpreted as recent contaminations. The individual peaks of the solid phase are inherited and can be detected in the liquid phase with lower intensity.

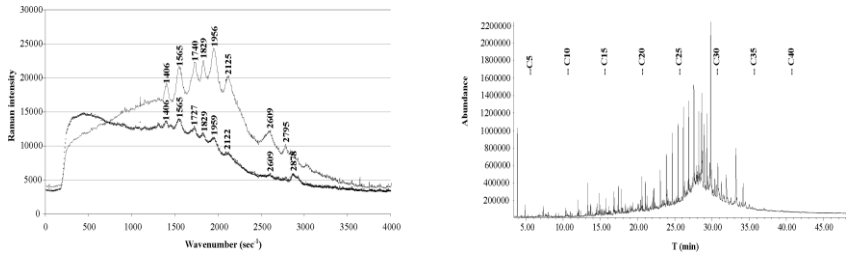

Fig. 16. The Raman peaks of the solid (1) and liqiud (2) phases (a); and gaschromatogram (b) of the sample C_{3-50}

In the case of the surface sample F2 GC analyses also detected alkanes with carbon atom number lower than C20 (Fig. 17). The Raman peaks of the liquid phase are much different here from the solid phase. Values from the solid phase are identical with those

mentioned above: 1,410 cm^{-1} (anthracene), 1,565 cm^{-1} asphaltene and C=C bond, 1,740 cm^{-1} C=O aliphatic aldehyds. In addition the 1,835 cm^{-1} C=C bond alkanes; at 1,962 and 2,128 cm^{-1} C≡C alkyne and alkyl acetylenes, at 2612 cm^{-1} refer to C=N bond, peak 2,795 cm^{-1} indicates O-CH_3. From the extract: 1,459 cm^{-1} isoparaffins, CH_2 2,850-3,000 cm^{-1} alkanes stretch, 1,317 cm^{-1} not identified exactly.

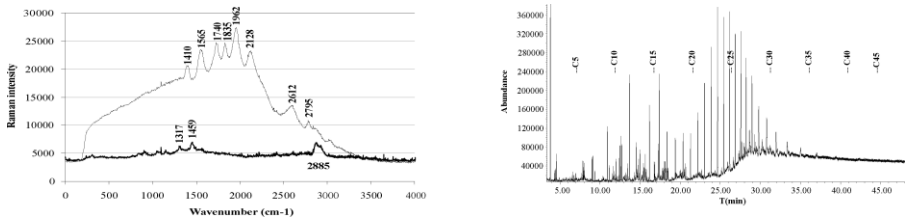

Fig. 17. The Raman peaks of the solid (1) and liqiud (2) phases (a); and gaschromatogram (b) of the sample F2

PHF is another sediment sampled from the stream channel (Fig. 18). The result shows that the stream is already polluted before reaching the industrial area. This is explained by communal pollution, garbage from the population, oil bottles as it was observed during fieldwork. Similarly, to sample F_2, also here several peaks are detectable in the province below C_{20}. At the Raman measurements, for the solid phase the characteristic peaks mentioned above are present. Alkine is detected at 2,128 cm^{-1}.

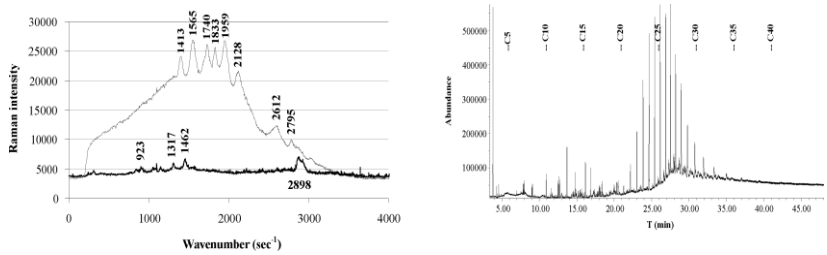

Fig. 18. The Raman peaks of the solid (1) and liqiud (2) phases (a); and gaschromatogram (b) of the sample PHF

Raman spectroscopy and GC-MS measurements allow the classification of hydrocarbon forms according to carbon atom number and coal bond types. Benzol ring structures, alkanes, alkenes and alkines could be identified. Alkylphenols, alkenes, characteristic C=C bonds (hydraulic oil, driving-gear oil, etc.) and alkines C≡C bonds. The distribution of the sample-sites which have the Raman peaks show that the artificial hydrocarbon contamination types are located around the centre of the former briquette factory, near the transformation station, pump stations, briquette-press and between the main buildings, such as the boiler house and the coal pillbox (Fig. 3) The main emission sites are found around the mazut tank and the pump station, which generates continuous pollution. Other places are also contaminated; however, we are unaware of any objects (tanks, lines, storage units, etc.) that could be the potential source of contamination. Presumably, the contamination did not reach the deeper subsurface layers due to the presence of a well-developed and thick marl aquitard.

Conclusion

The former briquette factory of Nagymányok is heavily contaminated by TPHs and heavy metals. The main contaminants are various hydrocarbons less amount are the heavy metals. For the classification of areas contaminated with heavy metal sin various degrees and variances cluster analysis was applied. Based on Ward's method (eucleidan distance) the partial areas are referred into four groups at the fourth level of hierarchy.

There are sites where the different artificial hydrocarbons were most commonly used. Heavier hydrocarbon type contamination has been proven in the majority of samples, and in some cases, diesel oil type contamination has also been found. Contamination types detected by Raman Spectroscopy results corroborate our findings obtained by the GC-MS analytical technique. The Raman peak evaluation based on fingerprint characterisation, where the peaks indicate single (C-C), double (C=C) and triple (C≡C) C-C bonds, i.e. alkanes, alkenes and alkines. In addition, benzol structures have been detected and, interpreting jointly with GC_MS results, the properties of pollution can be further refined. The qualitative classification of hydrocarbon pollutants, the interpretation of peaks, was promoted by the investigation of extracts in addition to the solid geological matrix.

Unfortunately, in reality the geological and the artificial bagrounds are rather variable, particularly in an industrial zone. Therefore, a selective extracting substance is advised to be employed in Raman spectroscopy. This substance should belong into the homologous series of hydrocarbon types, allows rapid and simple but reliable interpretation.

The environmental risks of the hydrocarbon groups identified by the mentioned bond types are different. Most dangerous to wildlife are the benzol ring structures and PAH compounds. Using rapid methods provides the opportunity to collect and evaluate larger amounts of samples which characterize the spatial distribution of the contaminated area.

Acknowledgements

Authors thanks to Nagymányok City Council for the financial support and thanks to RK Tech Ltd. for Balázs Domonkos for the Raman spectroscopy and for Dénes Lóczy (University of Pécs, Faculty of Sciences, Institute of Geography) and Kunsági-Máté Sándor (University of Pécs, Faculty of Sciences, (Department of General and Physical Chemistry) for his useful comments.

References

Ahern, M., Mullett, M., MacKay, C. & Hamilton, K. (2011). Residence in Coal-Mining Areas and Low-Birth-Weight Outcomes. Matern Child, *Health Journal* 15, 974–979.

Agarwal, U. P. (ed. T. Hu) (2008). *An Overview of Raman Spectroscopy as Applied to Lignocellulosic Materials, in Advances in Lignocellulosic Characterization*, USA: Blackwell Publishing.

Boadi, D. (2012). Decommissioning and Reclamation of Mine Sites, *International Journal of mining reclamation and environment*, 26, 91-92.

Bowden, S. A., Alabi, O. O., Edilbi, A., Brolly, C., Muirhead, D., Parnell, J. & Stacey, R. (2015). Asphaltene detection using surface enhanced Raman scattering (SERS), *Chem. Commun*. 51, 7152–7155.

Burke, E. J. A. (2001). Raman microspectrometry of fluid inclusions, *Lithos,* 55, 139–158.

Carlon, C (ed.) (2007). Derivation methods of soil screening values in Europe, A review and evaluation of national procedures towards harmonization. European Commission, Joint Research Centre, Ispra, EUR 22805-EN, 306.

Castiglioni, C., Tommasini, M. & Zerbi, G. L. (2004). Raman spectroscopy of poly conjugated molecules and materials: confinement effect in one and two dimensions, *Philosophical Transactions of the Royal Society of London A: Mathematical, Physical and Engineering Sciences*, 362(1824), 2425-2459.

Cicek, A. & Koparal, A. S. (2004). Accumulation of sulfur and heavy metals in soil and tree leaves sampled from the surroundings of Tunc¸bilek Thermal Power Plant, *Chemosphere*, 57, 1031–1036.

Cooper, J. B., Wise, K. L., Welch, W. T., Sumner, M. B., Wilt, B. K. & Bledsoe, R. R. (1997). Comparison of Near-IR, Raman, and Mid-IR Spectroscopies for the Determination of BTEX in Petroleum Fuels, *Applied Spectroscopy*, 51(11), 1613-1620.

David, C., Weindorf, Paulette, L. & Man, T. (2013). In-situ assessment of metal contamination via portable X-ray fluorescence spectroscopy: Zlatna, Romania, *Env. Poll.* 182, 92–100.

Decree of the Minister of the Environment and Water, Minister of Health and Minister of Agriculture No 6/2009. (IV.14.) KvVM-EüM-FVM

Decree No. 10/2000. (VI.2.) On quality standards of groundwater and geological agent protection. KöM-EüM-FVM-KHVM

Dick, D. P., Knicker, H., Avila, L., Inda, G., Giasson E. & Bissani, C. A. (2006). Organic matter in constructed soils from a coal mining area in southern Brazil, *Organic Geochemistry,* 37, 1537–1545.

Directive 2006/118/EC of the European Parliament and of the Council of 12 December 2006 on the protection of groundwater against pollution and deterioration (Daughter to 2000/60/EC)

Haas, J., Budai, T., Csontos, L., Fodor, L. & Konrád, K. (2010). *Magyarország pre-kainozoos földtani térképe 1:500000* (Pre-Cenozoic geological map of Hungary, 1:5000000), MÁFI Geological Institute of Hungary.

Haibin, L. & Zhenling, L. (2010). Recycling utilization patterns of coal mining waste in China, Resources, *Conservation and Recycling*, 54, 1331–1340.

Izake, E. L. (2010). Forensic and homeland security applications of modern portable Raman spectroscopy, *Forensic Science International*, 202, 1–8.

Kalnicky, D. J. & Singhvi, R. (2001). Field portable XRF analysis of environmental samples. *Journal of Hazardous Materials*, On-site Analysis. 83(1–2), 93–122.

Kelemen, S. R. & Fang, H. L. (2001). Maturity Trends in Raman Spectra from Kerogen and Coal, *Energy & Fuels*, 15, 653–658.

Kolomijeca, A., Kwon, Y. H., Sowoidnich, K., Prien, R. D., Schulz-Bull, D. E. & Kronfeldt, H. D. (2011). High Sensitive Raman Sensor for Continuous In-situ Detection of PAHs. *Proceedings of the Twenty-first International Offshore and Polar Engineering Conference*, Maui, Hawaii, USA, June 19-24.

Lambert, J. B., Shurvell, H. F. & Cooks, R. G. (1987). Introduction to organic spectroscopy, Macmillan.

Leyton, P., Sanchez-Cortes, S., Campos-Vallette, M., Domingo, C., Garcia-Ramos, J. V. & Saitz, C. (2005). Surface-Enhanced Micro-Raman Detection and Characterization of Calix[4]Arene–Polycyclic Aromatic Hydrocarbon Host–Guest Complexes, *Applied Spectroscopy*, 59(8), 1009-1015. PMID:16105209

Lyon, L. A., Keating, C. D., Fox, A. P., Baker, B. E., He, L., Nicewarner, S. R., Mulvaney, S. P. & Natan, M. J. (1998). *Raman Spectroscopy Analytical Chemistry,* 70(12), 341–361.

Lin-Vien, D., Colthup, N., Fateley, W. & Grasselli, J. (1991). The Handbook of Infrared and Raman Characteristic Frequencies of Organic Molecules, *Academic Press*, San Diego.

Lóczy, D., Czigány, Sz., Dezső, J., Gyenizse, P., Kovács, J., Nagyváradi, L. & Pirkhoffer, E. (2007). Geomorphological tasks in planning the rehabilitation of coal mining areas at Pécs, Hungary. *Geografia física e dinamica quaternaria,* 30, 203–207.

Nagy, E. (1971). Der unterliassiche Schichtenkomplex von Grestener Fazies im Mecsek-Gebirge (Ungarn), *Ann. Inst. Geol. Publ. Hung*, 54(2), 155-159.

Némedi, V. Z. (1987). Paläogeographische Verhältnisse während der Ablagerung der obertriassisch-unterliassischen Schichtenfolge im Mecsek-Gebirge (SO-Transdanubien), *Publ. Techn. Univ. Heavy Industry*, Miskolc, Ser. A. Mining, 43(1-4), 61-87.

Ökoproject Eger Ltd. (2008). MÁV Zrt Nagymányok Környezetvédelmi szűrővizsgálatok (Hungarian), National Railways Close Corporation Nagymányok (former Briquette Factory) *Environmental screening test. Manuscript*, MÁV, Pécs.

Panov, B. S., Dudik, A. M., Shevchenko O. A. & Matlak, E. S. (1999). On pollution of the biosphere in industrial areas: the example of the Donets coal Basin. *International Journal of Coal Geology,* 40, 199–210.

Pfannkuche, J., Lubecki, L., Schmidt, H., Kowalewska G. & Kronfeldt, H. D. (2012). The use of surface-enhanced Raman scattering (SERS) for detection of PAHs in the Gulf of Gdańsk (Baltic Sea), *Marine Pollution Bulletin*, 64, 614–626.

Powell, J., Jain, P., Bigger, A. & Townsend, T. Development and Application of a Framework to Examine the Occurrence of Hazardous Components in Discarded Construction and Demolition Debris: Case Study of Asbestos-Containing Material and Lead-Based Paint, J. Hazard. Toxic Radioact. Waste, 10.1061/(ASCE) HZ.2153-5515.0000266, 05015001

Rainbow, A. K. (ed) (1987). Reclamation, treatment and utilization of coal mining wastes, Rotterdam.

Raman database, Universitá Degli Studi di Parma, Departement of Physics and Earth Sciences, Italy, last visited on 27.01.2016. Retrieved from http://www.fis.unipr.it/phevix/ramandb.php

Schenzel, K. & Fischer, S. (2004). Applications of FT Raman spectroscopy for the characterisation of cellulose, *Lenzinger Berichte* 83, 64–70.

SDBS (Spectral Database for Organic Compounds), National Institute of Advanced Industrial Science and Technology (AIST),

Silva, S. L., Silva, A. M. S., Ribeirob, J., Martins, C. F. G., Da Silva, F. & Silva, C. (2011). Chromatographic and spectroscopic analysis of heavy crude oil mixtures with emphasis in nuclear magnetic resonance spectroscopy. *A review*. *Analytica Chimica Acta*, 707, 18–37.

Somos, L. (1965). A geological description of the Upper Triassic and of the coal bearing Lower Liassic Complex of the Mecsek mountains, *Acta Geol. Acad. Sci. Hung*., 9, 363–373.

Tanabe, K. & Hiraishi, J. Retrieved from http://sdbs.db.aist.go.jp/sdbs/cgi-bin/direct_frame_top.cgi last visisted: 29.01.2016.

Tommasini, M. & Zerbi, G. (2010). A theoretical Raman study on Polycyclic Aromatic Hydrocarbons of environmental interest. *Chemical Engineering Transactions,* 22, 263–268.

USDA (United States Department of Agriculture, Natural Resources Conservation Service) 2004: Soil survey laboratory methods manual. Version No. 4.0. Soil Survey Investigations Report No. 42.

Van Cott, R. J., McDonald, B. J. & Seelos, A. G. (1999). Standard soil sample preparation error and comparison of portable XRF to laboratory AA analytical results. *Nuclear Instruments and Methods in Physics Research Section A: Accelerators, Spectrometers, Detectors and Associated Equipment*, 422(1–3), 801–804.

Yenilmez, F., Kuter, N., Emil, M. K. & Aksoy, A. (2011). Evaluation of pollution levels at an abandoned coal mine site in Turkey with the aid of GIS, *International Journal of Coal Geology*, 86, 12–19.

Zemo, D., Bruya, J. E. & Graf, T. E. (1995). The application of petroleum hydrocarbon fingerprint characterization in site investigation and remediation, *Ground Water Monitoring and Remediation,* 15(2), 147–156.

Zhang, N., Tian, Z., Leng, Y., Wang, H., Song, F. & Meng, J. (2007). Raman characteristics of hydrocarbon and hydrocarbon inclusions. *Sci China Ser D-Earth Sci,* 50. 1171–1178.

József Denső[*], Amadé Halász[**], Viktória Poór[*], Dénes Lóczy[*]

[*] *Универзитет у Печују, ПМФ, Мађарска*
[**] *Универзитет у Печују, Медицински факултет, Мађарска*

ПРОВЕРА ЗАГАЂЕНОСТИ ИНДУСТРИЈСКОГ ЗЕМЉИШТА У СВРХУ ЊЕГОВОГ ОБНАВЉАЊА: ЕВАЛУАЦИЈА ОСНОВНИХ ГЕОЛОШКИХ ПОДАТАКА

Резиме: Истраживање у овом раду је засновано на резултатима брзе комбиноване мулти-технике у теренским мерењима под утицајем геолошког окружења које омогућава истраживање великих загађених подручја и даје подршку одлучивању. Истраживана област (бивша фабрика брикета у Нађимањоку) је веома контаминирана разним врстама бензенских угљоводоника. Садржај тешких метала је испитиван коришћењем GC-MS, турбидиметријске и Раман-спектроскопске методе, као и методом XRF. За квалитативну процену алкана, алкена и алкина, као и ароматичних једињења коришћена је Раманова анализа пикова. Области контаминиране хромом, цинком, кобалтом и канцерогеним угљоводоницима, у већини случајева апсорбују ове материје у угљеној прашини. Присуство хидрокарбоната у животној средини носи различите степене ризика, од којих су најопасније бензенске структуре и полициклични ароматични угљоводоници. Коришћење брзих метода обезбеђује могућност за сакупљање и евалуацију великог броја узорака који су просторно дистрибуирани у контаминираној области.